The Duffing oscillator: A precise electronic analog chaos demonstrator for the undergraduate laboratory

Article *in* American Journal of Physics · April 2001

DOI: 10.1119/1.1336838

CITATIONS
31

READS
3,570

2 authors, including:

Brian Keith Jones
Lancaster University
188 PUBLICATIONS **2,381** CITATIONS

SEE PROFILE

The Duffing oscillator: A precise electronic analog chaos demonstrator for the undergraduate laboratory

B. K. Jones[a] and G. Trefan
Department of Physics, Lancaster University, Lancaster LA1 4YB, United Kingdom

(Received 6 April 2000; accepted 24 May 2000)

A simple electronic circuit is described which can be used in the student laboratory to demonstrate and study nonlinear effects and chaos. The circuit shows the changes to the dynamical properties of the system with respect to three control parameters: the applied voltage amplitude and frequency and the circuit damping. The response voltage and its derivative can be displayed to give the phase space plot and the bifurcation diagram against any control parameter. The circuit is sufficiently ideal and stable to allow comparison of its analog output with the output obtained from standard digital computer simulations. As examples, the routes to chaos with respect to the control parameters and the bifurcation route to chaos, which follows the Feigenbaum scenario, are shown.
[DOI: 10.1119/1.1336838]

I. INTRODUCTION

When a dynamical system has an inherent instability, for example because of nonlinearity, its motion can become so erratic that for long enough times it becomes unpredictable. This noise-like motion of a deterministic dynamical system is referred to as chaotic motion.

Chaos was observed in electronic circuits in the early 20th century,[1] but its scientific significance became more apparent when the attempts at weather forecasting by computer simulations failed to produce reliable long-term predictions due to the chaotic character of the weather and the modeling equations.[2] Since then chaos has been found in many areas of science from astronomy through biology to electronic circuits[3–5] and materials.

One of the most frequently studied model dynamical systems that produces chaos is the Duffing oscillator.[6] Its popularity rests on its simplicity. It models in a one-dimensional space x a particle with mass m under a periodic external force $F\cos(2\pi ft+\phi)$ in a double well potential $U(x)$ with friction proportional to its actual velocity $-\alpha v=-\alpha\dot{x}$. Thus the equation of motion is

$$m\ddot{x}=-\mathrm{d}U(x)/\mathrm{d}x+F\cos(2\pi ft+\phi)-\alpha\dot{x} \tag{1a}$$

with

$$U(x)=-\tfrac{1}{2}(\mathrm{A}x^2)+\tfrac{1}{4}(\mathrm{B}x^4). \tag{1b}$$

The inherent instability, which is the cause of the chaos, is the hump of the potential $U(x)$ around its central symmetry point at $x=0$. Whenever the particle reaches this unstable point with nearly zero velocity a slight inbalance between the friction and the external force decides the further long-term course of the motion.

Because the Duffing oscillator is so simple, it can be studied analytically,[7] or by numerical simulations,[8–10] and one can also build an electrical circuit whose output voltage is a solution of Eq. (1), i.e., an analog computer.[7,11,12]

We note that the Duffing oscillator is not the simplest circuit to produce chaos.[13,14] Our goal here was to build a circuit which is simple enough to be available for a student laboratory to provide demonstrations of the basic textbook phenomena, shows a well-defined and obvious nonlinearity, and is accurate enough that its results can be compared with the results obtained by computer simulations or analytical investigations. As an extra advantage we have found that there are many possible effects to study including many which have not been reported in the literature.

To study the Duffing oscillator operating under a given set of control parameters, we must first characterize the motion in order to determine if it is regular, chaotic, or a mixture of both. In order to obtain information on the global character of the motion, it is enough to observe the motion in a reduced space, i.e., to create the so-called Poincaré surface of sections of the motion. The general technique in low-dimensional dynamical systems for creating the Poincaré surface of sections is to record all the coordinates in a properly chosen plane at which the phase-space trajectory intersects the plane from a given direction. This defines a set of points on the plane that is called the Poincaré surface of sections. The Poincaré surface of sections describes the dynamics fairly well. For example, if the Poincaré surface of sections shows a regular pattern, the motion is considered regular. If the Poincaré surface of sections shows no regularity, the motion is chaotic. If the Poincaré surface of sections consists of mixtures of regular patterns and one or more chaotic seas, the motion is considered a mixture of regular and chaotic motion with different degrees of chaoticity. Thus, if the regular patterns dominate in the Poincaré surface of sections, the motion is said to be weakly chaotic. The electronic way of obtaining the reduced dynamical description, i.e., the Poincaré surface of sections, is by sampling the output voltage, $V(t)$, with the sampling frequency, f, of the external driving force $F\cos(2\pi ft+\phi)$ at a fixed phase. The sampling results in a consecutive set of voltages. If these voltages trace a regular pattern, the Duffing oscillator is in a mode of regular motion, while if the sampled voltages are noise-like, the motion is chaotic. In this system the circuit noise is very small and cannot be detected directly. However, it is a general consequence of chaos theory that any disturbance, however small, will change the system trajectory (the butterfly effect).

The motion of a dynamical system such as the Duffing oscillator is studied in more detail generally by looking at its phase-space, i.e., plotting the velocity $v(t)=\dot{x}(t)$ versus $x(t)$. The electronic version of the phase-space plot is

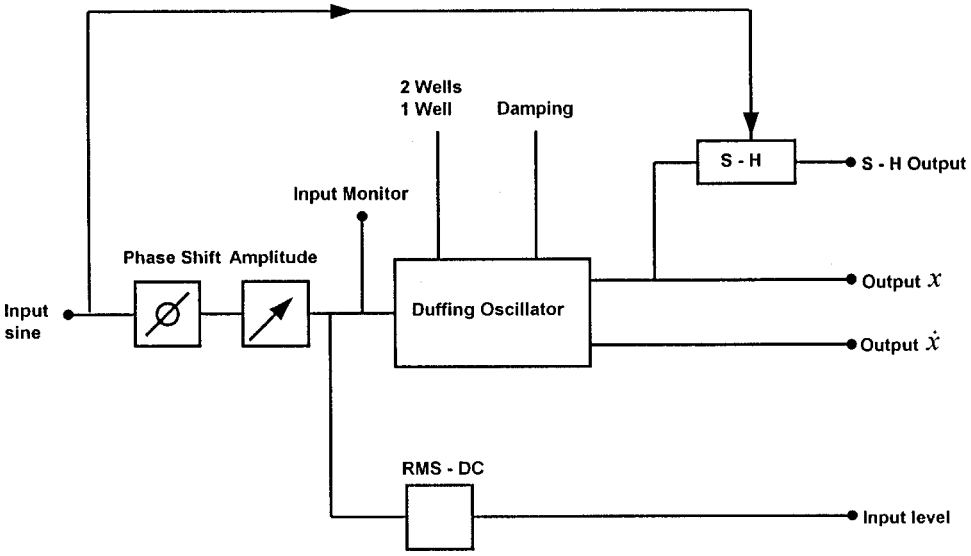

Fig. 1. Block diagram of the Duffing oscillator with its ancilliary circuits. The input sine signal is passed through a constant amplitude phase shifter and a digital precision amplitude controller to the Duffing oscillator. The output, x, and its derivative, $\dot{x}$, are passed to an oscilloscope to observe the phase space plot. The output, x, of the Duffing oscillator is observed by a sample-and-hold (S-H) circuit. In order to plot the bifurcation diagram with respect to the changing input voltage control parameter, this is detected with a precision rms to dc (ac-dc) converter.

readily available on a two-beam oscilloscope in the X-Y mode. Depending on the pattern of the phase-space picture the motion can be characterized.[13] For example, a phase-space pattern showing 1, 2, 4, etc. loops indicates regular motions of period 1, 2, 4, etc., while a scrambled phase-space indicates chaos. A further useful tool to characterize the motion is its spectrum, which is observed electronically by a spectrum analyzer. Regular motions are associated with discrete spectra of harmonics and subharmonics while chaos has a continuous spectrum. The mixture of discrete and continuous spectra indicates mixed motion, and the ratio of spectral powers of the discrete part to the continuous part indicates the degree of chaoticity of the motion.

This article describes an electronic circuit whose time-dependent output voltage $V(t)$ is proportional to the solution, x, of Eq. (1). The circuit is described in detail in Sec. II. In Sec. III, illustrations are given of the results of investigations on the Poincaré surface of sections, the phase-space plots, and the parameter space diagrams. These are compared with the results of computer simulations in the last section.

II. CIRCUIT DESCRIPTION

The block diagram of the circuit is shown in Fig. 1. The design consists of the following functional blocks: the input signal conditioning block, the Duffing oscillator analog computer circuit itself, and the output signal conditioning block. First the input sine signal is conditioned in order to control its amplitude and phase precisely, then the Duffing oscillator analog computer unit solves the equation of motion, and finally the conditioned output signal allows the user to observe the dynamical quantities of interest.

The input signal is derived from an external sine wave oscillator which is kept at constant amplitude and its frequency is monitored by a digital frequency meter. The input signal conditioning block consists of a constant amplitude phase shifter and a digital amplitude attenuator together with an ac-dc converter to give a measure of the signal size. Here we note only that the amplitude attenuator can control the amplitude with 0.3–4 mV rms accuracy for an amplitude of 3 V for the input signal $F\cos(2\pi ft+\phi)$. The use of this digital attenuator provides a very stable and reproducible setting which is important for good results from the system. The phase-shift is provided to make the display easier to interpret and its use will be described later. The precision ac-dc converter gives an analog measure of the input signal amplitude for use as a variable in displays or as a measure using a DVM.

The block diagram of the Duffing oscillator analog com-

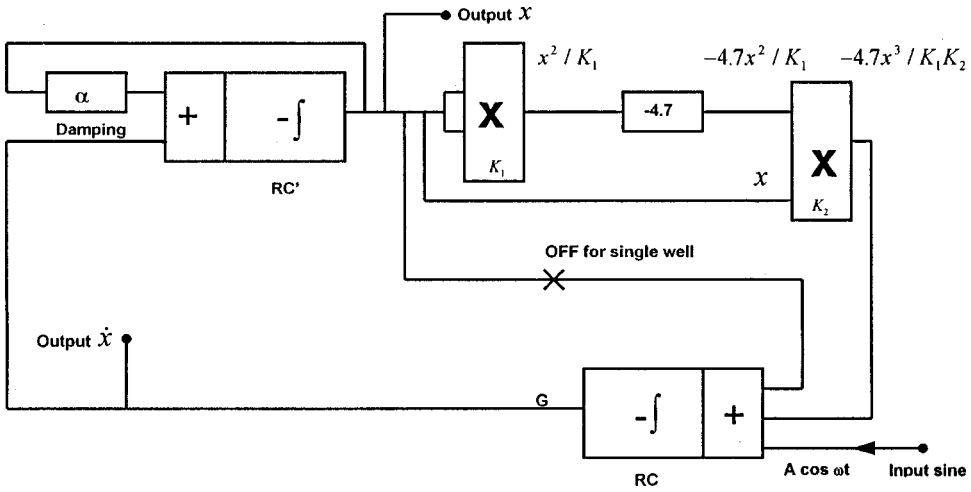

Fig. 2. The block diagram of the Duffing oscillator circuit itelf, i.e., the circuit that solves the Duffing equation (3). The nonlinear term is generated by two consecutive multiplications and the double integration is generated by two active integrators. There is also the addition of damping.

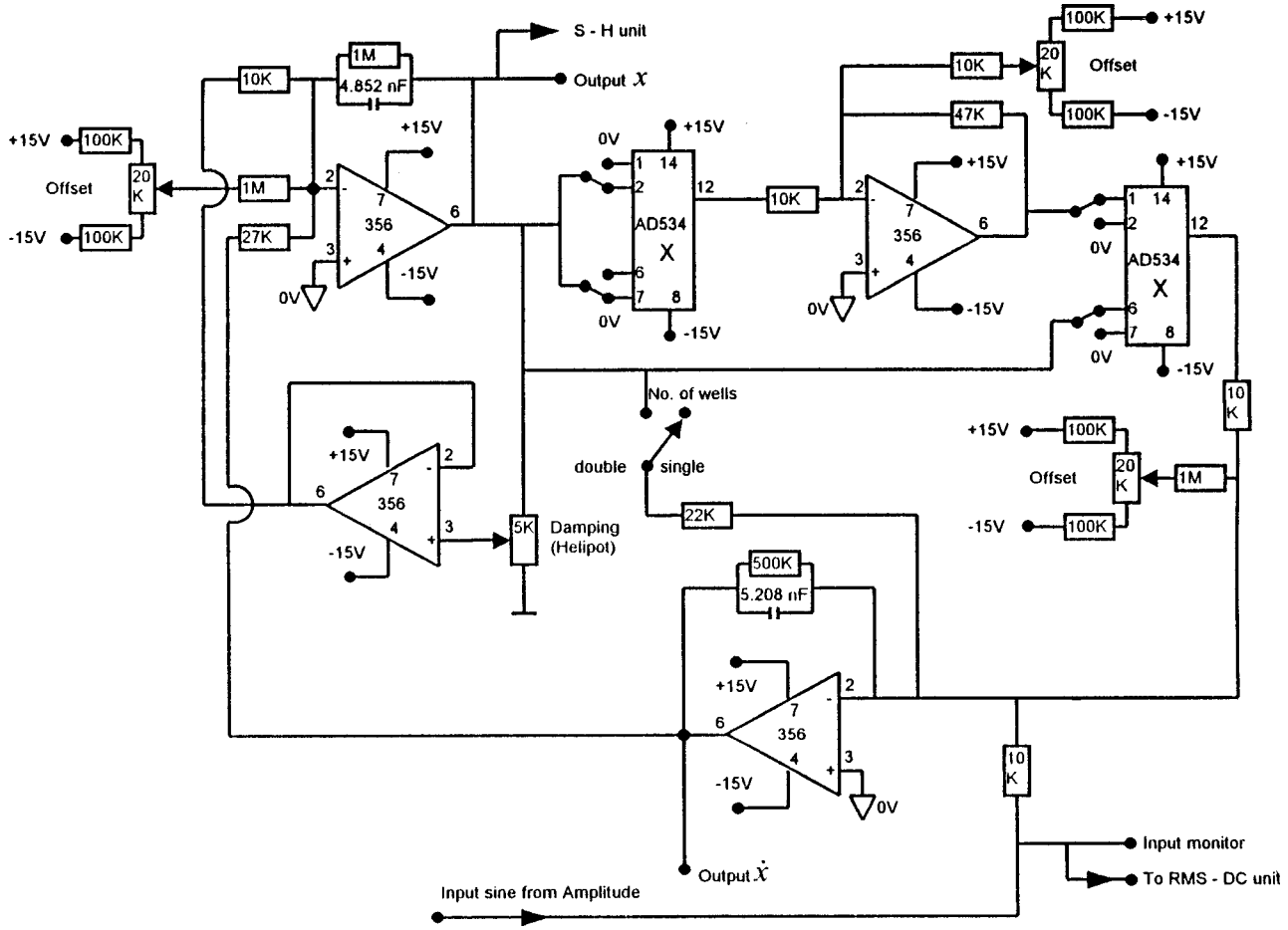

Fig. 3. Detailed circuit diagram of the Duffing oscillator. The integrators are built from low noise op-amps LF356, the multipliers are precision analog multipliers AD534, and the damping is applied using a precision helipot.

puter unit is shown in Fig. 2. It is a feedback loop. If we follow the signal from the bottom left corner on the block diagram, one can see that the precisely conditioned input signal $F\cos(2\pi ft+\phi)$ is added to the linear term x and the nonlinear term $-4.7x^3/\mathrm{K_1K_2}$ and is then integrated. Since this signal is the signal before final integration to become x, it is the time derivative $\dot{x}$ of the solution x. Adding, $-\alpha\dot{x}$ to signal $\dot{x}$ and integrating it again one obtains the solution x. The nonlinear component signal is gained from the two consecutive multiplications. The output signal conditioning block consists of the sample-and-hold (S-H) circuit.

The detailed circuit diagram of the Duffing oscillator analog computer unit is shown in Fig. 3. Starting the circuit analysis in the bottom left corner, one can see that the input signal $F\cos(2\pi ft+\phi)$ is added to the linear term x and the nonlinear term $-4.7x^3/\mathrm{K_1K_2}$ using an operational amplifier (op-amp) and is then integrated with a time constant RC, where $\mathrm{R}=10\,\mathrm{k}\Omega$ and $\mathrm{C}=5.21\,\mathrm{nF}$. The output of the previously mentioned op-amp yields the time derivative $\dot{x}$ of the solution x, since $\dot{x}$ is necessary to observe the phase-space signal and is therefore connected to a monitoring point. The signal $\dot{x}$ is led to another op-amp where it is added to the damping signal $-\alpha\dot{x}$ and is integrated with a time constant RC' where $\mathrm{R}=10\,\mathrm{k}\Omega$ and $\mathrm{C}'=4.85\,\mathrm{nF}$. The output of the second op-amp is the solution x. The nonlinear term is created from the solution x. First, a multiplier IC provides $x^2/\mathrm{K_1}$ where $\mathrm{K_1}$ is a present value. In our circuit it is set to $\mathrm{K_1}=10$. The signal $x^2/\mathrm{K_1}$ is amplified yielding $-4.7x^2/\mathrm{K_1}$, which is fed to a multiplier whose other input is x, thus yielding $-4.7x^3/\mathrm{K_1K_2}$, where $\mathrm{K_2}$ is a present value that we set to $\mathrm{K_2}=10$. We emphasize here that the circuit was designed to be a precise circuit so that the op-amps were carefully selected to be low-noise op-amps LF356. Note also that the damping signal $-\alpha\dot{x}$ is generated using a low-noise op-amp LF356 and it is variable using a precision helipot. The variability results in a value of α that can change from 0 to 1 with a precision of 0.001 read on the dial. The inductance of the wire-wound potentiometer may introduce small phase shifts which may prevent very high precision simulation. The multiplier ICs are precision analog multipliers AD534.

The equation of motion from the above circuit analysis is

$$\ddot{x}=-\alpha(\mathrm{RC}')^{-1}\dot{x}+(2.7\times 2.2\times \mathrm{RC}'\mathrm{RC}\times \mathrm{K_1K_2})^{-1}x-4.7(2.7\times \mathrm{RC}'\mathrm{RC}\times \mathrm{K_1K_2})^{-1}x^3+(\mathrm{RC}'\mathrm{RC})^{-1}F\cos(2\pi ft+\phi). \tag{2}$$

Substituting the actual values of $\mathrm{R}=10\,\mathrm{k}\Omega$, $\mathrm{C}=5.21\,\mathrm{nF}$, $\mathrm{C}'=4.85\,\mathrm{nF}$, and $\mathrm{K_1}=\mathrm{K_2}=10$, the equation of motion reads

$$\ddot{x}=-\alpha\times 2.06\times 10^4\dot{x}+0.666\times 10^8x-0.689\times 10^7x^3+3.95\times 10^8F\cos(2\pi ft+\phi). \tag{3}$$

The circuit analysis yields the natural frequency f_0 of the circuit. The natural frequency can be computed from Eq. (1)

since Eq. (1b) has two potential minima at positions $x_0 = \pm(A/B)^{1/2}$ and the natural frequency of the motion is the frequency f_0 of the small amplitude simple harmonic motion of a particle at the bottom of either of the potential wells. The two stable points can be seen by applying simple impulses to the input in order to switch the dc output level. The positions can be verified from the equations. The natural frequency f_0 is thus given from the second-order coefficient of the Taylor series expansion of potential given by Eq. (1b) around x_0 by $\frac{1}{2}(2\pi f_0)^2 = \frac{1}{2}[\mathrm{d}^2V/\mathrm{d}x^2]_{x_0}$. Since the second-order coefficient of the Taylor series expansion around x_0 is $[\mathrm{d}^2V/\mathrm{d}x^2]_{x_0} = 2\ \mathrm{A}$, the natural frequency is $f_0 = (2\ \mathrm{A})^{1/2}/2\pi$, which is $f_0 = 1.84\ \mathrm{kHz}$ in our circuit. The natural frequency f_0 can be measured by setting the damping coefficient to $\alpha = 0$, and with a low-input sine signal amplitude one changes the frequency from 0 to 5 kHz while observing the amplitude of the output signal. The frequency at which the amplitude reaches its highest value at the lowest input amplitude is the natural frequency. We found that at input voltages 0.15–0.2 V rms, the natural frequency is 1.83 kHz. The significance of determining the natural frequency lies in the fact that in exploring the dynamical responses of the Duffing oscillator fully, one has to investigate the output signal while keeping the drive signal frequency within separate dynamical regimes near, below, or above the natural frequency f_0.

III. RESULTS

During the experiments the output signals should be monitored for signs of saturation. By monitoring the output signal $V(t)$, proportional to x, and the applied input drive signal $F\cos(2\pi ft+\phi)$ before the phase shifter and attenuator on a double beam oscilloscope, one can compare their frequencies, amplitudes, and their phases. Similarly the time derivative $\dot{x}$ may be compared with the input signal. The oscilloscope is used in the X-Y (Lissajous) mode. The phase shift circuit has been incorporated to set a convenient relative phase between the input and output signals in order to clarify the pattern. The phase shift is frequency dependent so that it must only be used on the pure sine wave of the input signal. Monitoring the time derivative $\dot{V}(t)$ of the output signal versus $V(t)$ one observes the phase-space plot of the motion. The phase-space plot with 1 loop is a simple periodic motion or motion of period 1, with 2 loops period 2, with 4 loops period 4, etc. The phase-space plot with infinitely many loops we term chaos. We term the motion full chaos when the phase-space plot looks completely scrambled and weaker chaos when the phase-space plot consists of infinitely many loops sticking to a basin of attraction, the so-called strange attractor.

In order to double-check our interpretation of the character of the motion, we lead the output signal $V(t)$ to an analog spectrum analyser HP3582A. The spectrum of the motion of period 1 has a peak at frequency f, period 2 at frequency $f/2$, period 4 at frequency $f/4$, etc. Since it is a nonlinear circuit, there are also reflections of the spectrum at higher harmonics $2f$, $3f$, $4f$ etc. of the drive signal. The motion with full chaos has a continuous, although not constant, spectrum, while weaker chaos has a spectrum with definite peaks at frequencies, f, $f/2$, $f/4$, etc. emerging from the continuous background.

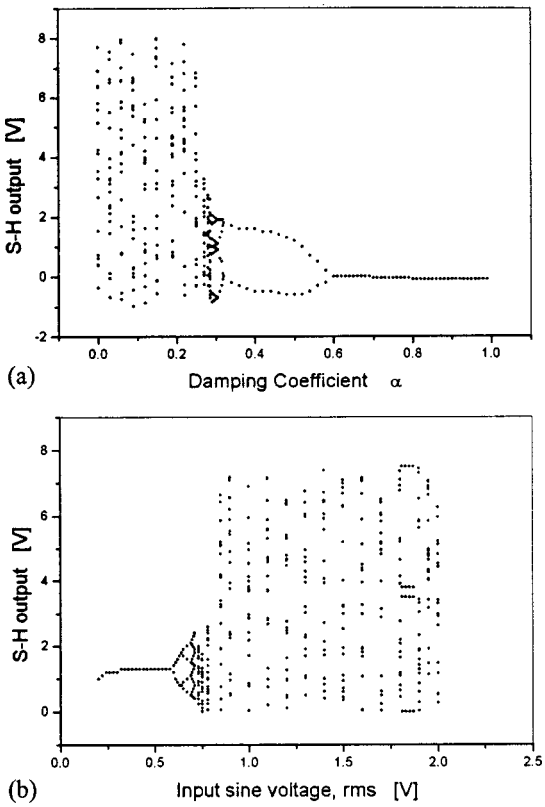

Fig. 4. Route to chaos via a period bifurcating cascade. (a) The two control parameters kept fixed are input voltage $F^* = 1.8$ V rms and frequency $f = 3.6$ kHz while the control parameter damping α changes from 0 to 1. (b) The two control parameters kept fixed are the input voltage frequency $f = 3.6$ kHz and damping parameter $\alpha = 0.11$ while changing control parameter input voltage F^* from 0.2 V rms to the level when the output signal is saturated at $F^* = 2.0$ V rms.

Since the output signal, i.e., the character of the motion, depends on the amplitude F and the frequency f of the external input signal $F\cos(2\pi ft+\phi)$, and on the damping coefficient α of the circuit, the parameters F, f, α are called control parameters.

The study of the circuit performance starts with fixing two out of the three control parameters and changing only one in order to observe how the character of the motion changes. For example, fix F and f, change α, and observe the character of the motion if it is periodic and with what period or chaotic fully or weakly. In order to do this efficiently, we use the built-in sample-and-hold circuit which samples the output signal $V(t)$ with the frequency f and phase ϕ of the external driving signal $F\cos(2\pi ft+\phi)$ so that for a motion of period 1 the sample-and-hold circuit gives one constant voltage, for a motion of period 2 it gives two distinct voltages, for a motion of period 4 it gives four distinct voltages, etc. For a chaotic motion it gives infinitely many voltages. Every distinct voltage appears a dot on the Y axis of the oscilloscope in the X-Y mode. Thus by sweeping the damping parameter, i.e., the control parameter, α, through all its possible values, we can observe how the character of the motion changes with respect to the damping. We found that keeping the rms input signal level $F^* = 1.8$ V rms and frequency $f = 3.6$ kHz while changing α from 1 to 0, the output voltage becomes chaotic via a consecutive period of bifurcations as shown in Fig. 4(a). From the values of α where consecutive bifurca-

tions occur, i.e., from $\alpha_1,\alpha_2,\alpha_3,\alpha_4,\ldots$, one builds up the first few elements of a series $\delta_1,\delta_2,\delta_3,\ldots$ defined by

$$\delta_1=(\alpha_2-\alpha_1)/(\alpha_3-\alpha_2), \quad \delta_2=(\alpha_3-\alpha_2)/(\alpha_4-\alpha_3). \tag{4}$$

Theoretically the series $\delta_1,\delta_2,\delta_3,\ldots$ converges to a universal number $\delta_{\text{inf}}=4.669\,20...$ independent of the dynamical details of the system.[15] From Fig. 4(b) we found that $\alpha_1=0.592$, $\alpha_2=0.648$, $\alpha_3=0.300$, and $\alpha_4=0.292$. From these values $\delta_1=1.14$ and $\delta_2=3.77$.

Since the input signal amplitude F is controlled digitally and stably, it can be changed in very small steps of about $\Delta F=0.3$–4 mV. This refinement allows us to investigate the character of the motion with respect to the control parameter F. Fixing $f=3.6$ kHz and $\alpha=0.11$ and sweeping with $F^*=F/(2)^{1/2}$ from 0.2 V rms to the level when the output signal $V(t)$ is saturated at $F^*=2.0$ V rms, we found that a period bifurcation cascade leading to chaos is followed by a set of period 4 motion near 1.8 V becoming chaotic again as shown in Fig. 4(b). The series of period doubling bifurcations $\delta_1,\delta_2,\delta_3,\ldots$ is built up from the control parameters $F_1,F_2,F_3,\ldots$ by

$$\delta_1=(F_2-F_1)/(F_3-F_2),$$
$$\delta_2=(F_3-F_2)/(F_4-F_3),\ldots. \tag{5}$$

We found from Fig. 4(b) that $F_1=0.600$, $F_2=0.318$, $F_3=0.300$, and $F_4=0.292$, and, correspondingly, $\delta_1=15.7$ and $\delta_2=2.25$. Again the consecutive series of δ_n should converge to $\delta_{\text{inf}}=4.669\,20...$. The values found for δ_{inf} in these two cases are reasonable in view of the restricted number of terms in the convergence. The reason for the limitation in the number of terms observed in this circuit is the poor noise in analog multipliers. They should be used with a large signal if possible. Note that for the latter example, the X voltage of the display can be taken from the ac-dc converter so that a direct display is possible. In this case the digital attenuator is set to full transfer and an analog potentiometer is used to slowly change the input signal amplitude. When the potentiometer is used as the control parameter, the bifurcation diagram needs to be plotted by hand.

A more informative way of presenting information about the character of the motion is to fix one of the control parameters out of the three and vary the other two control parameters while continuing to plot in symbols the character of the motion for every pair of the varied control parameters. In this way we build a two-dimensional ''topological'' plot which shows the regions of chaotic and regular motions. This two-dimensional plot is called the parameter space diagram. One of the advantages of the parameter space diagram is that it indicates different routes to chaos with respect to a changing control parameter, not only the route via consecutive bifurcations. In the example of Fig. 5(a), the parameter phase diagram obtained by keeping the damping coefficient α constant at $\alpha=0.11$ is plotted while the input rms amplitude F^* changes from $F^*=0.2$ V rms to $F^*=3.0$ V rms and the frequency of the input signal varies from 0.2 to 4 kHz. The regions of regular and chaotic motions are easily identified from their symbols. The parameter space diagram

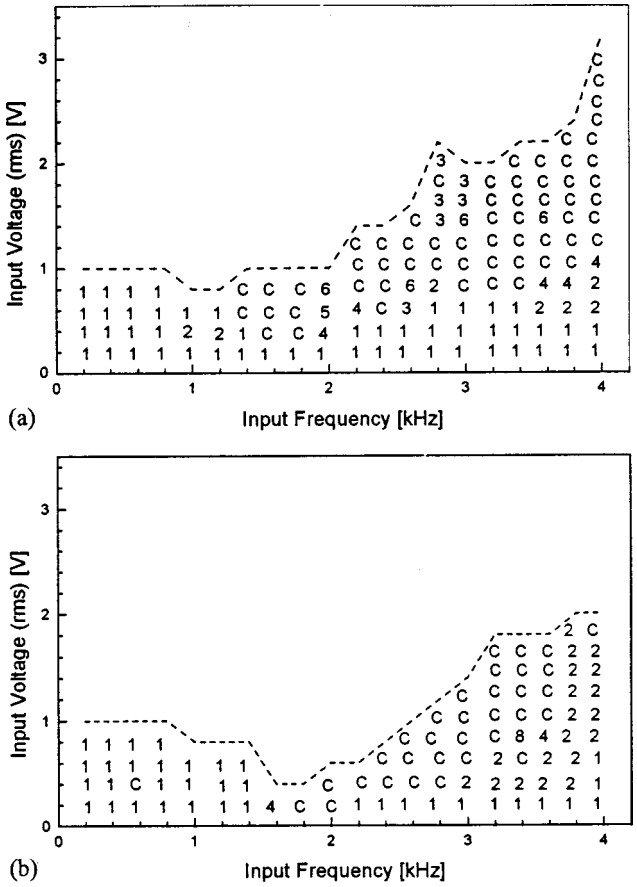

Fig. 5. Parameter space plots in which the damping coefficient is kept fixed at $\alpha=0.11$ while the input voltage F^* and its frequency f are changed. For parameters above the dashed line the circuit voltage level saturates at one or more places. The natural frequency of the circuit is 1.83 kHz. (a) Measured parameter space plot. (b) Computed parameter space plot. Key: C—chaotic, 1—period 1, 2—period 2, 4—period 4, etc. motion.

shows that for low-amplitude input signals the Duffing oscillator always executes a period 1 motion no matter what the driving frequency is. It also shows that for input driving frequencies well below the natural frequency, the Duffing oscillator typically follows the drive with a period 1 motion. When the Duffing oscillator is driven with a signal near to its natural frequency (1.84 kHz), it responds sensitively in the sense that for a very small change in any control parameter the character of the motion rapidly changes. One can also see from the parameter space plot that when the Duffing oscillator is driven with a signal of higher frequency than its natural frequency, for increasing input voltages it reaches chaos from period 1 motion typically via consecutive period bifurcations. It is also interesting to note that the borders of chaotic and regular motions are not sharply defined in the parameter space diagram.

The results shown in Fig. 5(b) show the computed parameter space diagram for the same values of the control parameters that were used in Fig. 5(a). We used the program package by Korsch *et al.*,[8] plotted the computed phase space data on the screen, and from this we decided the character of the motion. In order to use the program package, one has to rescale the equation of motion of Eq. (3). The rescaling rests on the idea that we measure the frequency in units of 10 kHz and measure the time in units of $\frac{1}{10}$ of a millisecond. With this rescaling the equation of motion Eq. (3) becomes

$$\ddot{x} = -\alpha \times 2.06\dot{x} + 0.666x - 0.0689x^3 + 5.60F^* \cos(2\pi f t + \phi), \quad (6)$$

where F^* denotes the rms of the input voltage signal measured in volts, and F^* is related to the input voltage amplitude F by $F = 2^{1/2}F^*$. We can see that Figs. 5(a) and 5(b) agree reasonably well in the sense that both parameter space plots have massive islands of chaotic motions and massive islands of regular motions for the same value of the control parameters. For such systems, very close agreement is unlikely since exactly comparable values are impossible to set in both systems.

The direct observation of this Duffing oscillator circuit demonstrates a few more interesting phenomena that we have not fully investigated and understood. At certain fixed control parameters ($F^* = 1.2$ V rms, $f = 4.0$ kHz, $\alpha = 0.11$), values of the output of the circuit alternate between chaotic and regular motion. It is not clear to us whether these sudden switches between chaotic and regular states of motion result from an intermittent chaos or are induced by electronic noise. We also found some hysteresis in the sense that when increasing a control parameter to cause the motion to go through consecutive bifurcations and chaos, the pattern is not reversible. When decreasing the same control parameter, the chaos to regular motion transition does not occur at the same value as the transition from regular to chaotic motion did on increasing the parameter.

IV. CONCLUSIONS

We have described a precise electronic circuit for realizing the Duffing oscillator analog computer. The electronic circuit is simple enough to be available for undergraduate laboratories and it is also precise enough to show many interesting phenomena of nonlinear dynamics. The experiment is liked by students.

There is considerable pedagogical value since instant and apparent demonstrations can be made of the basic principles on a real system. The basic behavior can be seen with a dc input signal and the system can be changed to one rather than two wells using the switch included. This removes the linear term in Eq. (3).

There are various ways of using the system for project work. We investigated the circuit behavior from the point of view of changing one control parameter only, thus obtaining a route to chaos. We found that the route to chaos from periodic motion when it occurs via a period doubling cascade follows the Feigenbaum scenario. We also investigated the circuit by changing two control parameters to build up a topological map of the motion in the so-called parameter space plot. We found that the parameter space plot is an informative representation of the motion in a global sense since it indicates non-period-bifurcating routes to chaos and it also indicates massive islands of parameter values of chaotic or regular motions. We compared our measured results with the results of computer simulations from a package easily available for an undergraduate laboratory and found a reasonable agreement between them. The power of the system is such that unreported effects can be readily seen and hence new research projects can be developed.

A few texts which have also been found to be of interest in the classroom are given, although not so directly relevant to the circuit used here.[16–25]

V. CIRCUIT DETAILS

Full circuit diagrams and suggestions for possible enhancements are available from the corresponding author.

ACKNOWLEDGMENTS

We would like to thank all the final year students who have helped with the project and D. H. Bidle and S. Ion for the electronic construction.

[a]Electronic mail: b.jones@lancaster.ac.uk

[1]B. van der Pol and J. van der Mark, ''Frequency demultiplication,'' Nature (London) **120**, 363–364 (1927).
[2]E. N. Lorenz, ''Deterministic non-periodic flow,'' J. Atmos. Sci. **20**, 130–141 (1963).
[3]J. M. A. Danby, *Celestial Mechanics* (Willman-Bell, Richmond, 1989).
[4]M. R. Guevara, L. Glass, and A. Shrier, ''Phase locking, period doubling bifurcations, and irregular dynamics in periodically stimulated cardiac cells,'' Science **214**, 1350–1353 (1981).
[5]L. O. Chua and R. N. Madan, ''Sights and sounds of chaos,'' IEEE Circuits Devices Mag. **4**, 3–13 (1988).
[6]G. Duffing, *Erzwungene Schwingung bei veränderlicher Eigenfrequenz und ihre technische Bedeutung* (Vieweg, Braunschweig, 1918).
[7]B. A. Hubermann and J. P. Crutchfield, ''Chaotic states of anharmonic systems in periodic fields,'' Phys. Rev. Lett. **43**, 1743–1747 (1979).
[8]H. J. Korsch and H.-J. Jodl, *Chaos—A Program Collection for the PC* (Springer Verlag, Berlin, 1994).
[9]R. Mannella, ''Computer experiments in non-linear stochastic physics,'' in *Noise in Nonlinear Dynamical Systems*, edited by F. Moss and P. V. E. McClintock (Cambridge U. P., Cambridge, 1989), pp. 189–217.
[10]T. S. Parker and L. O. Chua, *Practical Numerical Algorithms for Chaotic Systems* (Springer Verlag, Berlin, 1989).
[11]L. Fronzoni, ''Analogue simulations of stochastic processes by means of minimum component electronic devices,'' in *Chaos and Complexity*, edited by R. Livi, S. Ruffo, S. Ciliberto, and M. Buatti (World Scientific, Singapore, 1989), pp. 171–182.
[12]P. V. E. McClintock and F. Moss, ''Analogue techniques for the study of problems in stochastic nonlinear dynamics,'' in *Noise in Nonlinear Dynamical Systems*, edited by F. Moss and P. V. E. McClintock (Cambridge U. P., Cambridge, 1989), pp. 243–277.
[13]T. P. Weldon, ''An inductorless double scroll chaotic circuit,'' Am. J. Phys. **58**, 936–941 (1990).
[14]T. Matsumoto, ''Chaos in electronic circuits,'' Proc. IEEE **75**, 1033–1057 (1987).
[15]M. J. Feigenbaum, ''Quantitative universality for a class of nonlinear transformations,'' J. Stat. Phys. **19**, 25–52 (1980).
[16]F. C. Moon, *Chaotic Vibrations: An Introduction for Applied Scientists and Engineers* (Wiley, New York, 1987).
[17]A. B. Pippard, *Response and Stability* (Cambridge U. P., Cambridge, 1985).
[18]I. Stewart, *Does God Play Dice*? (Penguin, London, 1990).
[19]M. Schroeder, *Fractals, Chaos, Power Laws* (Freeman, New York, 1991).
[20]H-O. Peitgen, H. Jurgens, and D. Saupe, *Fractals for the Classroom*, Parts 1 and 2 with activities books (Springer-Verlag, New York, 1991, in conjunction with NCTM).
[21]H-G. Schuster, *Deterministic Chaos* (VCH, Weinheim, 1984).
[22]E. A. Jackson, *Perspectives of Nonlinear Dynamics*, Vols. 1, 2 (Cambridge U. P., Cambridge, 1989–1990).
[23]B. B. Mandelbrot, *The Fractal Geometry of Nature* (Freeman, New York, 1977).
[24]J. Feder, *Fractals* (Plenum, New York, 1988).
[25]A. Bunde and S. Havlin (eds.), *Fractals and Disordered Systems* (Springer-Verlag, Berlin, 1996).